JOURNAL OF MATERIALS SCIENCE **39** (2004) 5755–5763

Novel terbium-zircon yellow pigment

J. K. KAR*, R. STEVENS, C. R. BOWEN
Material Research Centre, Department of Engineering and Applied Science, University of Bath, Bath, BA2 7AY, UK
E-mail: jiten_kar@hotmail.com

The incorporation of the terbium oxide into the zircon host lattice in the presence of different types (NaF and LiF) and amounts (2 and 5 wt%) of mineralisers created various shades of yellow at several calcination temperatures with 2 h soaking time. The shade of yellow observed was primarily a lemon yellow, different from existing Pr-Zircon yellow. The pigment powders were characterised using techniques such as XRD, SEM, Particle Size Analysis and Spectrophotometry. From the X-ray diffraction patterns, zircon was found to be the major phase present together with small amounts of un-reacted zirconia. The amount of un-reacted zirconia in each case was calculated using an external standard method. SEM micrographs of the samples indicated growth of the tetrahedral shaped crystals improved on addition of sodium fluoride. The same zircon crystals were observed to form with the use of lithium fluoride as a mineraliser, but the shape of the crystals differed. The average particle size was found to vary between 11–15 μm. Stability of these pigment powders was tested in an unleaded commercial transparent glaze. Yellow coloured glazed tiles were produced suggesting that the pigments were stable in the commercial unleaded transparent glaze. Colour measurements were performed on the pigment powder samples and on the coloured glazed tiles.

1. Introduction

Production of ceramics is one of the enduring ancient arts. Early potters ceramicist used strong colouring compounds such as the natural minerals containing Co, Cr, Fe and Mn as the colouring agents. However, it was not possible to continue use of these minerals under industrial conditions because of the instability of their composition in the processes involved. Subsequently, colouring agents based on synthetic inorganic pigments have been developed. The pigments in the host lattice belonging to the zircon group $ZrO_2 \cdot SiO_2$, which crystallise in the tetragonal system, show a wide colour palette. Based on these, ceramic colours having light blue, light green, yellow and orange tones can be obtained [1]. These Zircon colours are of commercial significance in the production of under-glaze ceramic decoration.

Several yellow colours are already available commercially for various ceramic decoration applications. They include zirconia-vanadium, tin-vanadium and praseodymium yellow etc. Zirconia-vanadium yellows can be prepared by calcining zirconium oxide with small amounts of ammonium metavanadate [2–5]. Titanium or iron oxide may be used to alter the shade. In the absence of these compounds, lemon yellow is obtained and in their presence, an orange yellow colour is generated. In ceramic coatings zirconia-vanadium yellows are often weaker in colour than the tin-vanadium yellows and rather muddier than praseodymium-zircon yellows. However they are economical stains for use in both zinc containing or zinc free glazes and give a strong colour in low-lead, low-boron glazes. The primary deterrent to the use of tin-vanadium yellows however is not for any technical deficiency but is due to the high cost of tin oxide, which is a major component of the precursor mixture.

Praseodymium-zircon pigments can be formed by calcination of 5% praseodymium oxide with a stoichiometric mixture of zirconium oxide and silica in the presence of mineralisers to produce a bright yellow pigment [6–8]. These pigments have excellent tinting strength in high temperature coatings and can be used in almost all ceramic coatings preferably with a zircon opacifier. The pigments are being used increasingly for applications in which the firing temperature exceeds 1000°C.

This paper presents the processing and characterisation of the novel terbium doped zircon pigment and describes its possible use in high temperature ceramic applications.

2. Experimental procedure

2.1. Sample preparation

Several processing methods are available for the preparation of pigments. In this research work, oxides, in varying predetermined amounts have been homogeneously and ionically interdiffused to form a crystalline

*Author to whom all correspondence should be addressed.

TABLE I Composition, flux agents and precursors for the samples.

Sample name	Formula $Zr_{(1-x)}Tb_xSiO_4$	Mineraliser (added wt% of the total mixture)		Calcination temperature (°C)
		Type	wt (%)	
ZSTB	$X = 0.05$	NaF	2	1150
ZSTB1	$X = 0.05$	NaF	2	1250
ZSTB2	$X = 0.05$	NaF	5	1150
ZSTB3	$X = 0.05$	NaF	5	1250
ZSTB4	$X = 0.05$	NaF	5	1450
ZSTB5	$X = 0.05$	LiF	2	1150
ZSTB6	$X = 0.05$	LiF	2	1250
ZSTB7	$X = 0.05$	LiF	5	1150
ZSTB8	$X = 0.025$	NaF	5	1150
ZSTB9	$X = 0.1$	NaF	5	1150

matrix of a chromophore agent, which forms the basis of the ceramic pigment.

The chemical compositions of the samples prepared are given in the Table I. The Precursors used were ZrO_2, SiO_2, and Tb_4O_7. NaF and LiF were added as mineralisers to form the host lattice zircon at lower calcination temperatures. Various shades of yellow colour were observed after calcination at different temperatures with a 2 h soaking time.

2.2. Characterisation methods

2.2.1. X-ray diffraction

XRD analyses of the samples were undertaken using a Philips PW1730/00 diffractometer using monochromatic Cu K_α radiation, $\lambda = 0.154060$ nm. X-ray scans were made between 2θ angles of 10° and 80°.

Equation 1, given below was used for the quantitative investigation of the phases [9].

$$\frac{I_\alpha}{I_{\alpha p}} = \frac{w_\alpha\left(\frac{\mu_\alpha}{\rho_\alpha}\right)}{w_\alpha\left(\frac{\mu_\alpha}{\rho_\alpha} - \frac{\mu_\beta}{\rho_\beta}\right) + \frac{\mu_\beta}{\rho_\beta}} \quad (1)$$

where I_α = Intensity of the ZrO_2 peak in the mixture, $I_{\alpha p}$ = Intensity of the pure ZrO_2 peak, w_α = Weight fraction of the un-reacted ZrO_2 to be calculated, μ_α/ρ_α = Mass absorption coefficient of ZrO_2, μ_β/ρ_β = Mass absorption coefficient of $ZrSiO_4$, μ_α and μ_β = Linear absorption coefficient of ZrO_2 and $ZrSiO_4$ respectively, and ρ_α and ρ_β = Density of ZrO_2 and $ZrSiO_4$ respectively.

The mass absorption coefficient for ZrO_2 and $ZrSiO_4$ can be calculated using the Equation 2 given below.

$$\mu = \frac{n}{V_c}\sum(\mu_a)_I \quad (2)$$

where n = Number of molecules in the unit cell of the compound, V_c = Volume of the unit cell.
and

$$\sum(\mu_a)_I \rightarrow \left(\frac{\mu}{\rho}\right)_i\left(\frac{A}{N}\right)$$

where $(\frac{\mu}{\rho})_i$ = mass absorption coefficient of the individual element using Cu K_α radiation, A = atomic number of the element and N = Avogadro's number = 6.023×10^{23}.

The values of the mass absorption coefficient of $ZrSiO_4$ and ZrO_2 were calculated to be 176.6 and 275 respectively.

The values of the mass absorption coefficient of the individual elements used in Equation 2 to calculate the mass absorption coefficient of the compound were obtained from the "International Tables for X-ray Crystallography" [10].

2.2.2. Scanning electron microscopy

Scanning electron microscopy in combination with energy dispersive X-ray analysis was used in this study. A Jeol JSM-6310 analytical scanning electron microscope fitted with a 10/85-link microanalysis system manufactured by Oxford Instrument was used in the experiments.

2.2.3. Particle size

There are several techniques for particle size characterisation such as sedimentation, laser diffraction, microscopy, sieving and X-ray diffraction which can be utilised [11]. Each characterisation method measures a different property of the particle (maximum length, minimum length, volume, surface area etc.) and therefore gives a different result compared with the other techniques. The quoted particle sizes of the samples were measured using a Malvern particle size analyser (Mastersizer X) based on a laser scattering technique.

2.2.4. Application of the pigment in the glaze and colour measurement

Stability of each of the pigments was tested in a commercial transparent leadless glaze. Glazes were coloured by adding 8 wt% of the pigment to the glaze. Intimate mixing was achieved by milling the materials constituting the slip, for half an hour in a high-density plastic container using zirconia/alumina grinding media. This treatment gave a homogeneous mixture of the pigment and glaze. The ground mixtures were then sieved through a 100 μm mesh. A spray gun was used to apply the stained ceramic glazes to standard test tiles.

The optimum results were achieved when the mass of glaze deposited was between 0.15–0.2 gm/cm^2.

Firing was carried out in a Carbolite furnace using the conditions below:

Step 1—100°C/h to 120°C, soaking time 2 h
Step 2—100°C/h to 600°C soaking time 1 h
Step 3—100°C/h to 1070°C soaking time 2 h
Step 4—Furnace cooling

Colour measurements were carried out on the fired pigment powders and coloured glazed tiles using a Spectraflash SF600 plus spectrophotometer. The colour coordinates $L^*a^*b^*$ define the colour of a sample in a uniform colour space, where L^*—Lightness axis, for white $L^* = 100$ and 0 for black, a^*—Red-Green axis, positive means red and negative means green, b^*—Yellow-Blue axis, positive means yellow and negative means blue.

3. Results and discussion

3.1. X-ray diffraction

The samples, which produced coloration after various heat treatment combinations were examined by XRD. The XRD traces of the samples are given in Figs 1 to 6. The Miller indices of the major peaks are also given adjacent to the peaks.

Figs 1 to 6 represent the X-ray diffraction patterns of the samples obtained with different types and amounts of mineraliser and fired at various calcination temperatures.

Diffraction patterns of the samples (Fig. 1) were obtained with LiF as a mineraliser. From the diffraction patterns, it can be seen that at 1150 and 1250°C, most of the peaks can be attributed to zircon although traces of zirconia are detected. However it was also interesting to note that the amount of LiF had an effect on the relative amount of each phase present in the sample. Larger ZrO_2 peaks were observed when 5% LiF

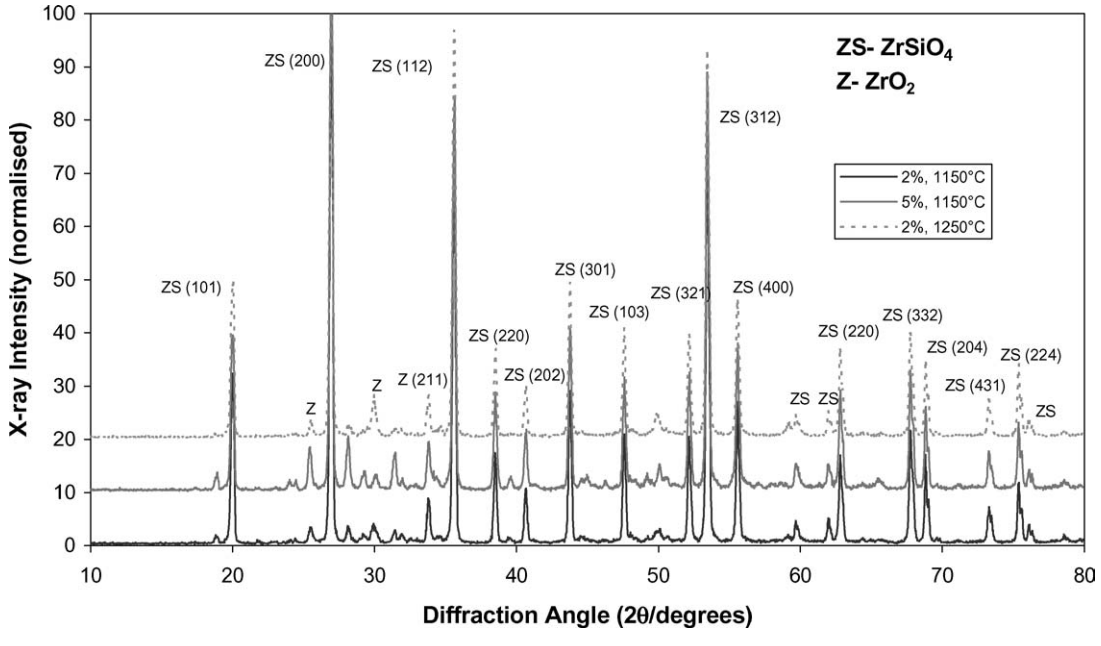

Figure 1 X-ray diffraction patterns of the pigment powders $Zr_{(1-x)}Tb_xSiO_4$ ($x = 0.05$) with 2 and 5% LiF and calcined at different calcination temperatures (1150 and 1250°C).

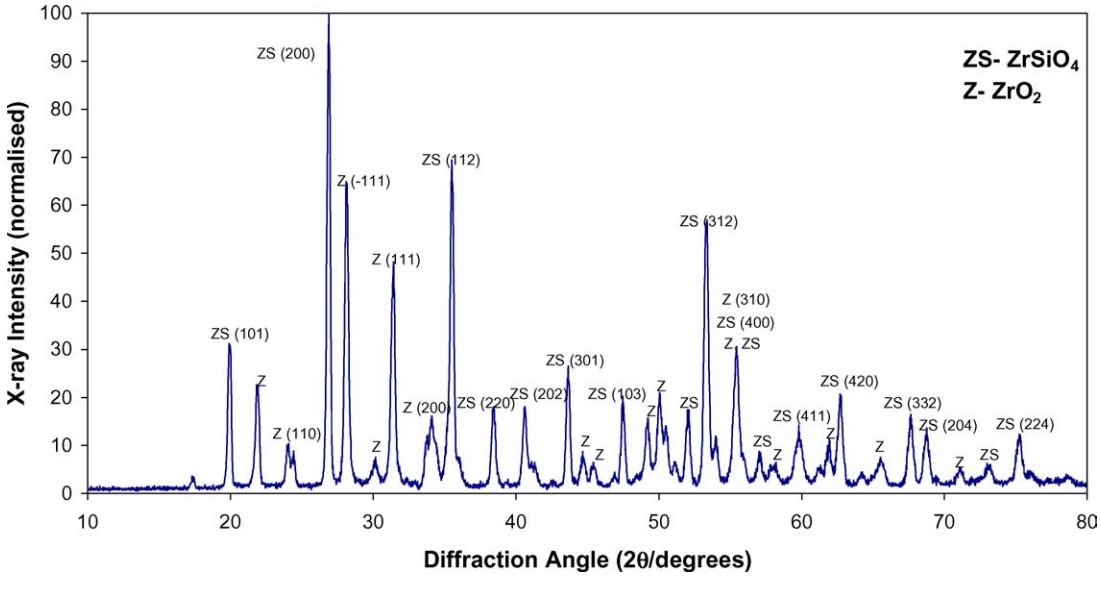

Figure 2 X-ray diffraction pattern of the pigment powder ZSTB {$x = 0.05$, NaF (2%), 1150°C}.

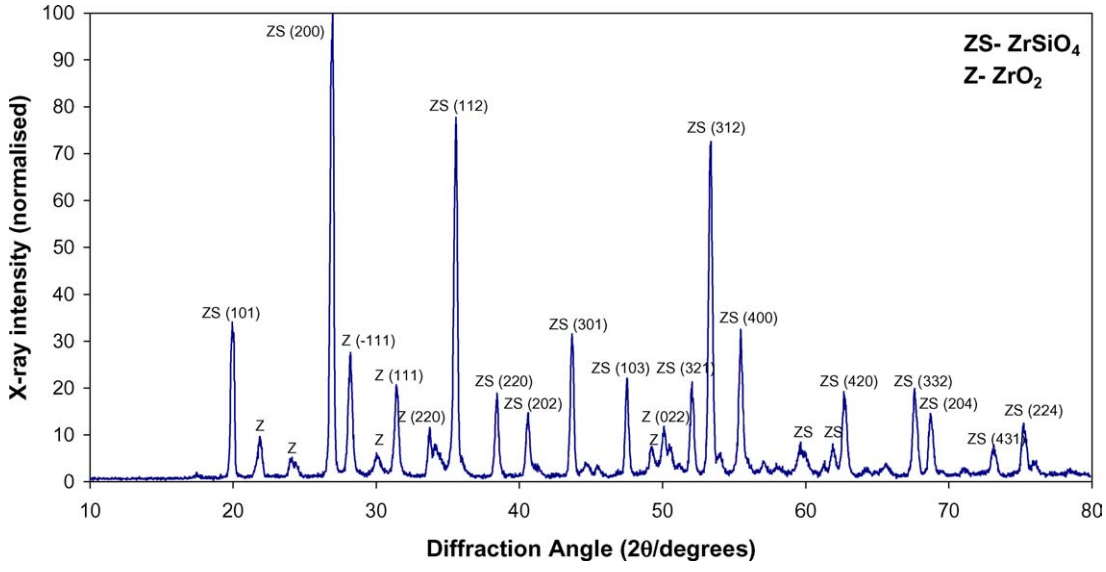

Figure 3 X-ray diffraction pattern of the pigment powder ZSTB1 ($x = 0.05$, NaF (2%), 1250°C}.

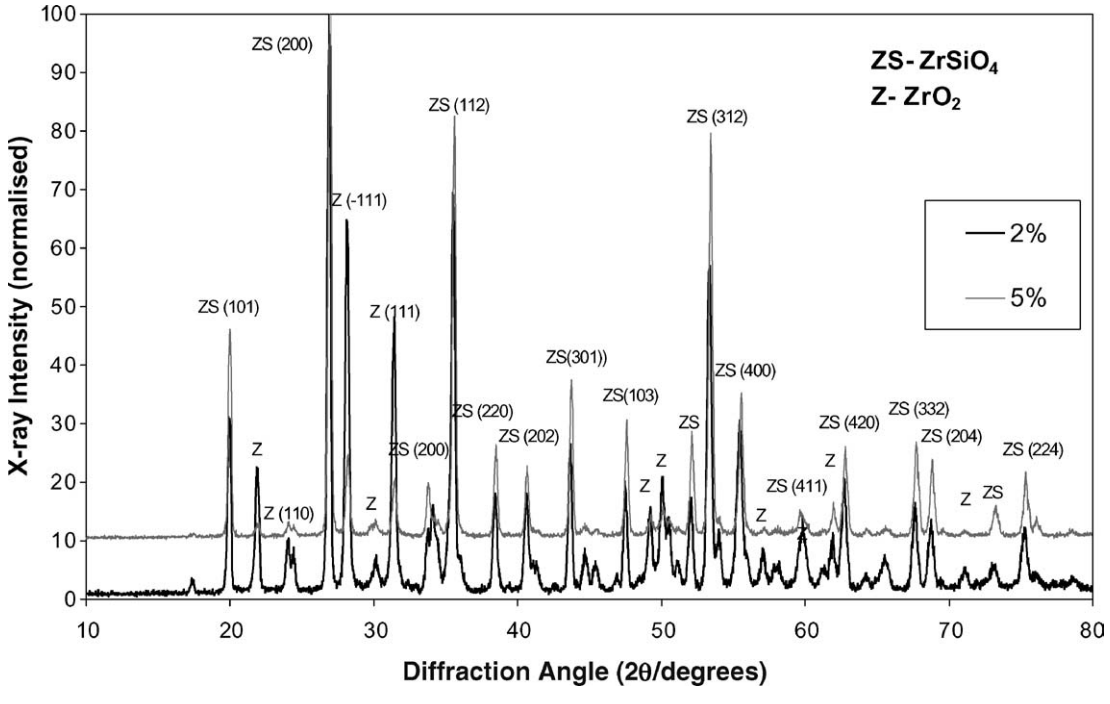

Figure 4 X-ray diffraction patterns of the pigment powders $Zr_{(1-x)}Tb_xSiO_4$ ($x = 0.05$) with NaF (2 and 5%) and calcined at the same temperature (1150°C).

was used compared to 2% LiF and calcined at the same temperature (1150°C).

XRD patterns of the sample with NaF as the mineraliser (Figs 2 and 3) revealed the presence of two different phases, $ZrSiO_4$ and ZrO_2. The ZrO_2 peaks were higher at 1150°C (Fig. 2) compared with 1250°C (Fig. 3) indicating the effect of temperature on the relative amount of phases present in the sample. This indicates that at higher temperature ZrO_2 combines with SiO_2 to form zircon and hence affects the relative amount of the phases, $ZrSiO_4$ and ZrO_2, present. Less intense peaks for ZrO_2 were observed at 1150°C and 5% NaF compared with 1150°C and 2% NaF shown in (Fig. 4) demonstrating the significant effect of the amount of added mineraliser on the phase concentration in the sample.

It is interesting to note that similar diffraction patterns were obtained by increasing the temperature from 1150 to 1250°C (Fig. 5) using 5% NaF as a mineraliser. A further increase in temperature to 1450°C did not have any effect on the phases, as shown in Fig. 5 indicating that liquid formation had taken place at the lowest temperature.

Similar diffraction patterns were observed with increase in the concentration of the colouring oxide (terbium oxide), Fig. 6. The XRD patterns of the samples (Figs 1 to 6) showed that no compounds other than $ZrSiO_4$ and ZrO_2 were detected; it is suggested that almost all of the Tb_4O_7 added had been

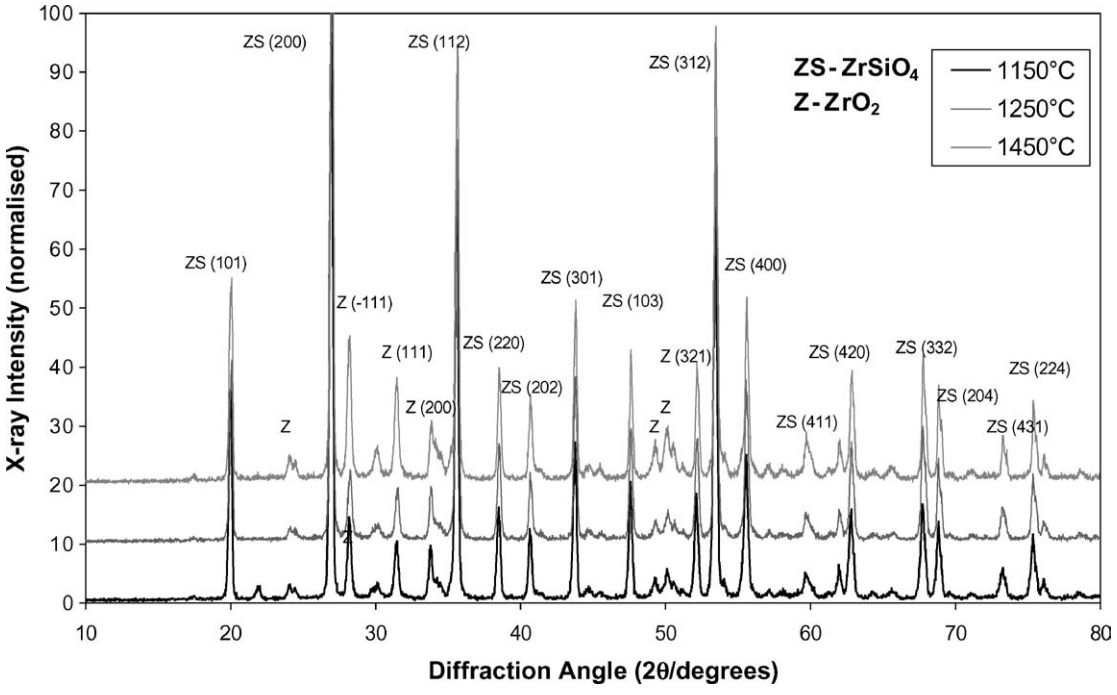

Figure 5 X-ray diffraction patterns of the pigment powders $Zr_{(1-x)}Tb_xSiO_4$ ($x = 0.05$) with NaF (5%) and calcined at various calcination temperatures (1150, 1250 and 1450°C).

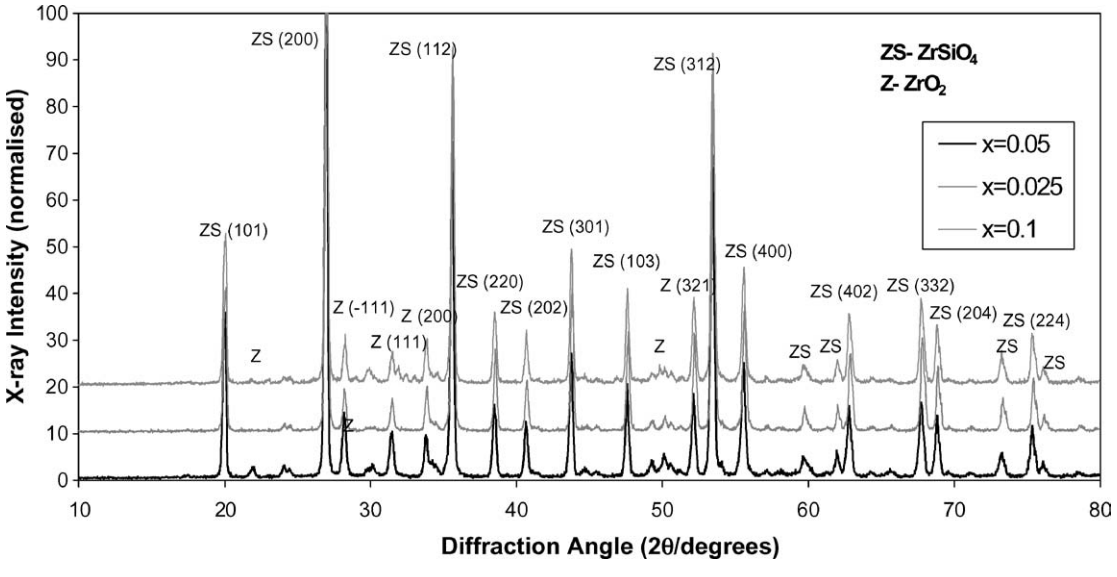

Figure 6 X-ray diffraction patterns of the pigment powders $Zr_{(1-x)}Tb_xSiO_4$ ($x = 0.025, 0.05, 0.1$) with NaF (5%) mineraliser and calcined at 1150°C.

incorporated into the zircon structure to form a solid solution.

3.1.1. Calculation of the lattice parameters and volume of the unit cell

The crystal structure of zircon is tetragonal. The change of lattice parameters a and c with the amount of chromophore ions for Tb-zircon pigment obtained at the heat treatment temperature of 1150°C is given in Table II.

From Table II, it is apparent that an increase in the concentration of the colouring oxide increases the "a" value whereas the "c" value decreases. The unit cell size (volume) decreases with an increase in the concentration of the colouring oxide.

The weight fraction of the un-reacted zirconia present in the calcined samples was calculated using Equation 1 and the results are summarised in Table III.

From the Fig. 7, it is seen that the value of the weight fraction in the case of NaF (2%), 1150°C was higher compared to NaF (5%), 1150°C indicating the presence of larger amounts of the un-reacted zirconia in the 2%

TABLE II Change of lattice parameters and unit cell volume with the amount of Tb content for Tb-zircon pigment heat-treated at 1150°C

$Zr_{(1-x)}Tb_xSiO_4$	a (Å)	c (Å)	Volume of the unit cell (Å)^3
$X = 0.025$	6.59494	6.06673	263.86170
$X = 0.05$	6.61897	5.96974	261.53886
$X = 0.1$	6.62934	5.92275	260.29389

TABLE III Weight fraction of the un-reacted zirconia present in various samples

Sample name	Weight fraction of un-reacted zirconia
$Zr_{(1-x)}Tb_xSiO_4(x = 0.05)$, NaF (2%), 1150°C	0.236
$Zr_{(1-x)}Tb_xSiO_4(x = 0.05)$, NaF (5%), 1150°C	0.085
$Zr_{(1-x)}Tb_xSiO_4(x = 0.025)$, NaF (5%), 1150°C	0.061
$Zr_{(1-x)}Tb_xSiO_4(x = 0.1)$, NaF (5%), 1150°C	0.060
$Zr_{(1-x)}Tb_xSiO_4(x = 0.05)$, LiF (2%), 1150°C	0.025
$Zr_{(1-x)}Tb_xSiO_4(x = 0.05)$, LiF (2%), 1250°C	0.018
$Zr_{(1-x)}Tb_xSiO_4(x = 0.05)$, LiF (5%), 1150°C	0.060

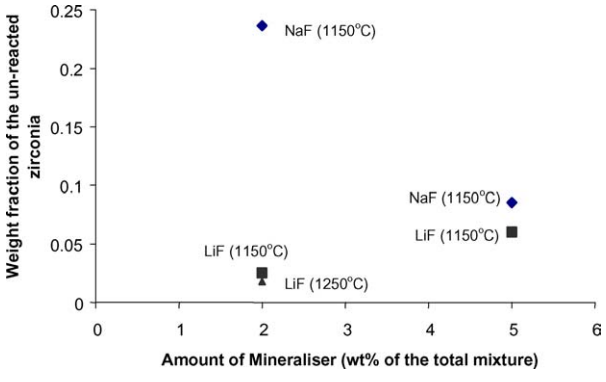

Figure 7 Weight fraction of the un-reacted zirconia present in the samples($Zr_{1-x}Tb_xSiO_4, x = 0.05$) at different calcination temperatures, with the addition of various types and amounts of mineraliser

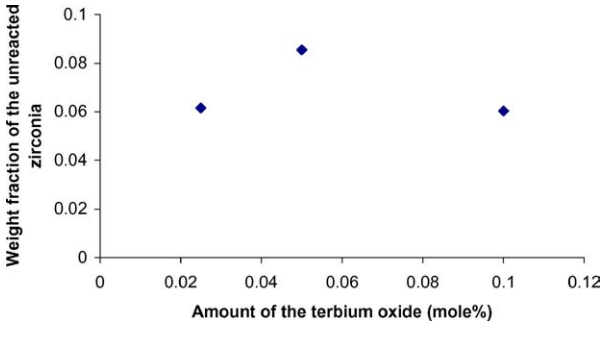

Figure 8 Graphical representation of the effect of the increasing content of the terbium on the weight fraction of the un-reacted zirconia present in the samples ($Zr_{1-x}Tb_xSiO_4$, $x = 0.025$, 0.5 and 0.1) at 1150°C (NaF = 5%).

addition compared to 5% NaF. However, with LiF, a larger amount of un-reacted zirconia was observed for the 5% addition compared to 2% addition when calcined at the same temperature (1150°C). Increasing the temperature to 1250°C when 2% LiF was used as a mineraliser did not affect the amount of un-reacted zirconia appreciably.

The weight fraction of the un-reacted zirconia has been augmented by increasing the concentration of the terbium from 0.025 to 0.05, it then decreased for 0.1 addition (Fig. 8). The reason for this behaviour is not easily explained due to the unavailablity of the $ZrSiO_4$-Tb_4O_7 phase diagram.

3.2. Measurement of surface morphology and appearance using SEM

The structure and morphology of the Tb-Zircon samples were examined using the scanning electron microscope. SEM images of the samples at different temperature are given in Figs 9 to 11.

SEM micrographs of the samples (Figs 9 and 10) indicated the growth of the tetrahedral shaped crystal, improved by the addition of sodium fluoride as mineraliser. Large amounts of un-reacted zirconia were found to be present in the sample when 2% of mineraliser was added (Fig. 9) compared to 5% (Fig. 11), which is in good agreement with the XRD data.

The same zircon crystals were observed to form by the use of lithium fluoride as a mineraliser (Fig. 10) but the shape of crystals differed. The difference in morphology can be attributed to the different in interfacial energies of the mineralisers and crystals [12].

TABLE IV Particle sizes of various samples obtained after different calcination temperatures, defined in Table I (After 3 h ball milling)

Sample name	Particle sizes (μm)		
	d (0.5)	d (0.1)	d (0.9)
ZSTB	11.44	3.65	24.36
ZSTB1	13.50	5.33	28.87
ZSTB2	14.11	5.77	27.40
ZSTB3	14.25	4.75	33.32
ZSTB4	14.58	4.34	37.70
ZSTB5	12.05	5.05	23.97
ZSTB6	12.32	4.92	27.92
ZSTB7	13.04	4.10	33.57
ZSTB8	12.27	4.71	22.25
ZSTB9	10.98	4.05	20.11

3.3. Particle size

The pigment powders obtained after calcination at various temperature were subjected to grinding for 3 h in a high-density plastic container with zirconia grinding media using water as the suspension liquid. Particle size measurements of the powders was then undertaken using the laser diffraction technique; the results are given in Table IV:

(a) The average particle size is increased with the increase in temperature from 1150°C to 1250°C when both NaF (2%) and LiF (2%) were used as mineraliser.

(b) Increasing the amount of NaF and LiF to 5% at the same temperature 1150°C also increased the average particle size.

(c) There is an increase in the average particle size on increasing the temperature from 1150 to 1250°C and then to 1450°C, when NaF (5%) was used.

(d) Increasing the concentration of terbium from 0.025 to 0.05 increased the average particle size, subsequently decreased for the 0.1 addition.

3.4. Colour measurement

Colour measurements were carried out on the fired pigment powders and coloured glazed tiles using a spectrophotometer. The colour coordinates L^*, a^* and b^*, which define the colour of the sample are given in the Tables V and VI.

Pigment powders ZSTB5, ZSTB6 and ZSTB7 were manufactured with LiF as a mineraliser. Lemon yellow

TABLE V $L^*a^*b^*$ parameters of the $Zr_{(1-x)}Tb_xSiO_4$ ($x = 0.05$) pigment powders and pigments in glaze with different mineraliser and calcination temperatures

	Pigment powders			Pigments in glaze		
Symbol	L^*	a^*	b^*	L^*	a^*	b^*
ZSTB	94.60	−6.62	35.37	86.48	−6.26	64.84
ZSTB1	95.46	−7.13	29.04	87.12	−7.60	59.57
ZSTB2	93.20	−8.03	47.73	86.44	−6.75	65.75
ZSTB3	93.92	−8.54	44.05	86.30	−8.11	60.50
ZSTB4	92.21	−5.26	42.73	86.65	−7.79	56.03
ZSTB5	91.99	−6.31	47.06	87.57	−8.14	57.17
ZSTB6	91.9	−6.37	43.83	87.53	−8.18	54.16
ZSTB7	90.33	−3.02	42.88	87.22	−7.31	52.50

colours were observed both for the powders and the coloured glaze tiles. The value of b^* was at a maximum for the sample ZSTB5 and decreased for the sample ZSTB6 and ZSTB7 respectively both for the isolated powder and when in the glaze, Table V. The increase in the value of b^* leads to an increase in the intensity of the yellow colour.

In the glaze, for samples (LiF = 2%), both b^* and a^* values decreased with the increase in temperature from 1150 to 1250°C (ZSTB5 and ZSTB6). A further decrease in the a^* value and a slight increase in b^* value was observed using 5% LiF calcined at 1150°C (ZSTB7).

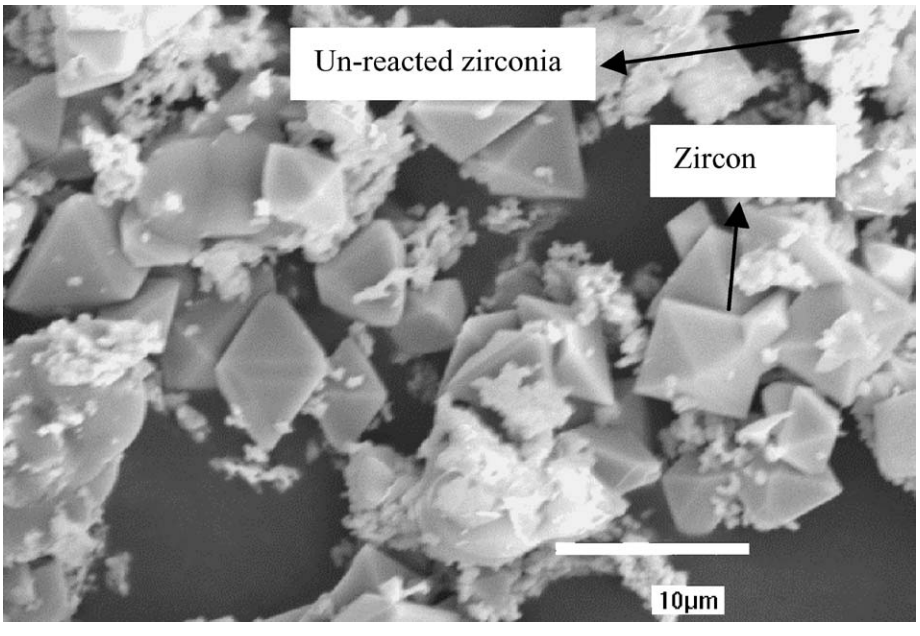

Figure 9 SEM micrograph of the sample ZSTB {NaF (2%), 1150°C}, ×2700.

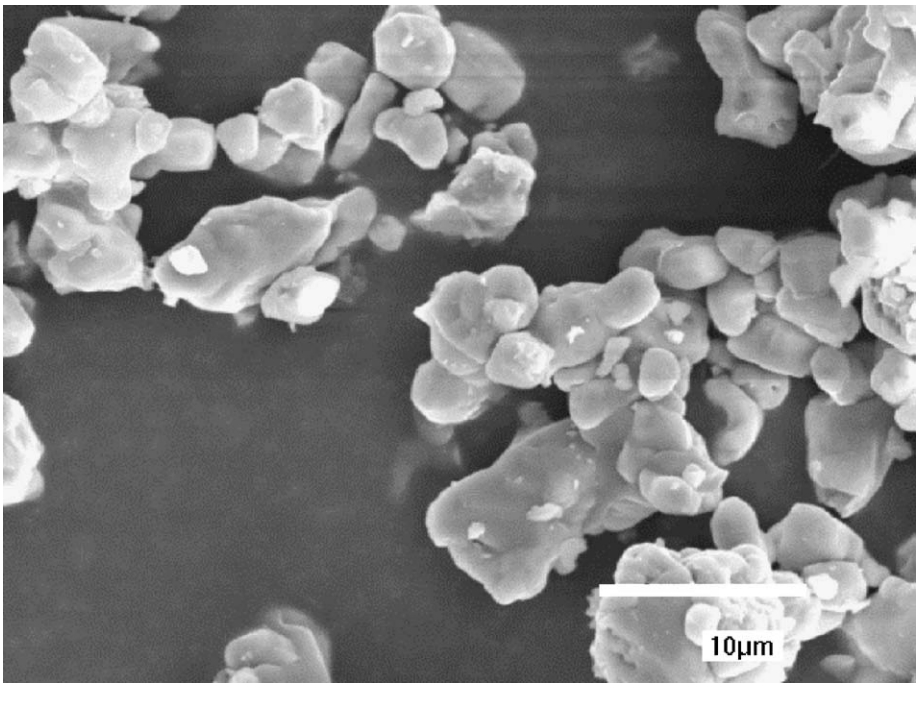

Figure 10 SEM micrograph of the sample ZSTB5 {LiF (2%), 1150°C}, ×2700.

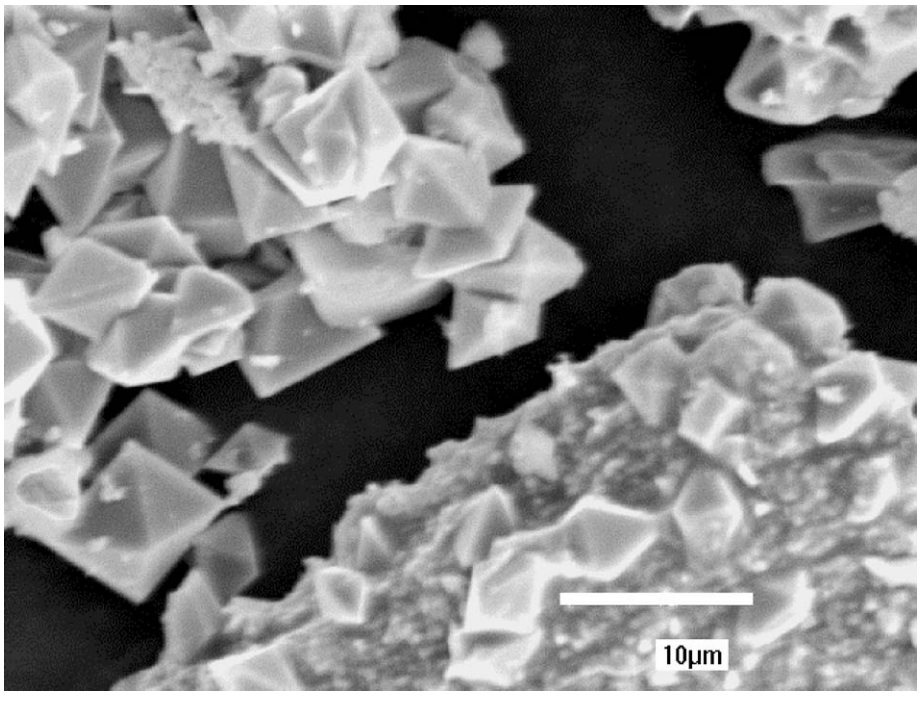

Figure 11 SEM micrograph of the sample ZSTB2 {NaF (5%), 1150°C}, ×2700.

Deep yellow colours were observed in the case of the samples ZSTB, ZSTB1, ZSTB2, ZSTB3 and ZSTB4 obtained with NaF. These powders gave a strong yellow colour when incorporated in the glaze.

When present in the glaze, for 2% NaF, b^* and a^* values were decreased with the increase in temperature from 1150 to 1250°C. Increasing the amount to 5% and using a calcination at 1150°C increased both the a^* and b^* values. There was a decrease in the b^* value with an increase in temperature from 1150 to 1450°C, but no regular trend was noticed in the case of the a^* values when NaF (5%) was used as a mineraliser.

Colours were less intense in the powder form when compared to the coloured glaze tiles in all cases, which was evident from the a^* and b^* values. This was due to the fact that the remnant zirconia reacted with silica (from the glaze) to form zircon, producing a more intense colour.

Increasing the concentration of the terbium oxide from 2.5 to 5% increased the b^* value but a further increase in concentration to 10% did not affect the intensity of the colour appreciably. Similarly increasing the concentration of terbium oxide decreases the a^* and L^* values as shown in the Table VI.

The mechanism of the colour formation in the Tb-Zircon pigment can be explained on the basis of crystal field splitting [13, 14]. Interaction of the terbium oxide with the host lattice zircon gives rise to splitting of the f orbitals into two groups, one group having higher energy and the other group having lower energy, similar to the transition metal oxides. The transition energy from the higher energy level to the lower level gives the characteristic colour to the compound. Electro-neutrality is achieved by two means, anionic deficiency in the lattice or partial replacement of oxygen by fluorine anions with the use of mineralisers NaF or LiF. In the first case it acts only as a fluxing agent whereas in the second case it plays a structural role. The NaF or LiF are used as mineralisers to form the lattice at lower calcination temperatures, enabling the formation of liquid phases at lower reaction temperatures.

TABLE VI The effect of the increasing content of the terbium on the colour hue of the $Zr_{(1-x)}Tb_xSiO_4$ pigment using $L^*a^*b^*$ coordinates (only at a firing temperature of 1150°C)

	Pigment powders			Pigments in glaze		
Symbol	L^*	a^*	b^*	L^*	a^*	b^*
ZSTB8	93.62	−8.12	49.16	86.94	−8.19	59.32
ZSTB2	93.20	−8.03	47.73	86.44	−7.25	65.75
ZSTB9	91.40	−6.96	57.77	86.15	−7.15	66.09

4. Conclusions

1. Various shades of yellow (different from the Pr-Zircon yellow) were observed when terbium oxide was incorporated into the zircon host lattice. The variation in shade is considered due to the presence of different types and amounts of mineraliser, calcined at various temperatures.

2. X-ray diffraction was used to identify different phases. In most cases Zircon was found to be the major phase with small amounts of un-reacted zirconia still present. It was difficult to achieve the complete formation of zircon even at higher temperatures and when different types and amounts of mineraliser were used.

3. XRD traces of the samples indicated compounds other than $ZrSiO_4$ and ZrO_2 were not present. Hence it is suggested that the added Tb_4O_7 has been incorporated into the zircon structure to form a solid solution.

4. SEM micrographs of the samples indicated the growth of tetrahedral shaped crystals (zircon). Large amounts of un-reacted zirconia were found to be present in the sample when 2% mineraliser was added compared to 5%, which was in good agreement with the

results obtained from XRD. The same zircon crystals were observed when lithium fluoride was used as a mineraliser, but the shape of the crystals was different.

5. Average particle sizes were increased with the increase in the temperature and amount of mineraliser. Increasing the concentration of terbium from 0.025 to 0.05 increased the average particle size and which decreased for additions above 0.1. Above the 0.1 volume fraction the particle size decreased.

6. Increasing the concentration of the terbium oxide from 2.5 to 5% increased the b^* value (hence changed the colour shade) but a further increase in concentration to 10% did not affect the intensity of the colour appreciably.

Acknowledgments

The authors are grateful to the European Commission for providing financial assistance and to Treibacher AUERMET, Austria for supply of the materials.

References

1. E. SH. KHARASHVILI, *Glass Ceram.* **42** (1985) 459.
2. F. T. BOOTH and G. N. PEEL, *Trans. British Ceram. Soc.* **61** (1962) 359.
3. C. DECKER, *Ceram. Eng. Sci. Proc.* **11** (1990) 307.
4. J. BRETKA, R. G. BOWMAN and T. BROWN, *J. Aust. Ceram. Soc.* **17** (1981) 37.
5. C. A. SEABRIGHT and H. C. DRAKER, *Amer. Ceram. Soc. Bull.* **40** (1961) 1.
6. R. A. EPPLER, *Ind. Eng. Chem. Prod. Res. Develop.*, **10** (1971) 352.
7. F. BONDIOLI, A. B. CORRADI, A. M. FERRARI and T. MANFREDINI, *J. Amer. Ceram. Soc.* **83** (2000) 1518.
8. E. H. RAY, T. D CARNAHAN and R. M. SULLLIVAN, *Amer. Ceram. Soc. Bull.* **40** (1961) 13.
9. B. D. CULLITY, "Elements of X-ray Diffraction," 2nd ed. (Addison-Wesley, London, 1978).
10. The International Union of Crystallography, "International Tables for X-ray Crystallography" (Kynoch Press, Birmingham, UK, 1962) p. 162.
11. T. ALLEN, "Particle Size Measurement" (Chapman and Hall, London, 1992).
12. YET-MING CHIANG, DUNBAR BIRNICK III and W. D. KINGERY, "Physical Ceramics: Principles of Ceramic Science and Engineering" (John Wiley and Sons, Inc., NY, 1997) p. 351.
13. K. NASSAU, "The Physics and Chemistry of Color (The Fifteen Causes of Color)" (John Wiley and Sons, 1983) p. 23.
14. R. TILLEY, "Colour and Optical Properties of Materials" (John Wiley and Sons, Ltd 1999) p. 155.

Received 24 July 2003
and accepted 13 May 2004